Eur. Phys. J. D **20**, 77–86 (2002)
DOI: 10.1140/epjd/e2002-00120-5

THE EUROPEAN PHYSICAL JOURNAL D

Formation of Cs_2 molecules via Feshbach resonances stabilized by spontaneous emission: theoretical treatment with the Fourier grid method

P. Pellegrini, O. Dulieu, and F. Masnou-Seeuws[a]

Laboratoire Aimé Cotton, CNRS, bâtiment 505, Campus d'Orsay, 91405 Orsay Cedex, France

Received 14 February 2002
Published online 28 June 2002

Abstract. This paper proposes a general method to investigate Feshbach resonances in atomic collisions similar to Cs($6s$) + Cs($6p$) in the thermal or cold regime. In order to compute the predissociation widths of the $C^1\Pi_u(6s+5d)$ bound vibrational levels of Cs_2, coupled both with the $(2)^3\Sigma_u^+(6s+6p)$ continuum and with the $(2)^3\Pi_u(6s+5d)$ vibrational series, a Fourier grid method is implemented, with an optical potential. A convenient way of optimizing the latter is proposed. A large number of resonances are found and calculations of their cross-sections for stabilization into ground state molecules show that the rate may be important. This confirms the interpretation of Lintz and Bouchiat [Phys. Rev. Lett. **80**, 2570 (1998)] who observed dimer formation in cell experiments. Possible generalization to the cold regime relies on the possibility to tune the position of a resonance to coincide with the maximum of the collisional energy distribution.

PACS. 33.80.Gj Diffuse spectra; predissociation, photodissociation – 34.10.+x General theories and models of atomic and molecular collisions and interactions (including statistical theories, transition state, stochastic and trajectory models, etc.) – 34.50.-s Scattering of atoms and molecules – 03.65.Ge Solutions of wave equations: bound states – 02.70.Jn Collocation methods

1 Introduction

The formation of molecules *via* photoassociation in a cold atomic sample has received much attention lately [1–4]. In the photoassociation reaction [5], two colliding alkali atoms absorb a photon red-detuned relative to the resonance line, populating a bound vibrational level in an excited molecular potential curve. This molecule then decays by spontaneous emission, usually giving back a pair of free atoms and therefore dissociating. It can be stabilized into a long-lived ground-state molecule only in some particular situations, where the branching ratio of bound-bound transitions is non-negligible as compared to bound-continuum transitions. Schemes to stabilize photoassociated molecules are therefore actively investigated.

One such scheme has been discussed recently for the Cs_2 molecule [6], and relies upon resonant coupling between two vibrational series in the excited state. In the chosen example, a vibrational level close to the dissociation limit of the $0_u^+(6s+6p_{1/2})$ curve is populated *via* photoassociation of two colliding ground state atoms, and the population transferred to a vibrational level of the narrower $0_u^+(6s+6p_{3/2})$ curve, which has a better Franck-Condon overlap with the bound levels of the ground state. The excited molecule can thus be stabilized by spontaneous emission. An obvious generalization of such a scheme would be to excite directly one atom, and consider a Feshbach resonance [7] in the scattering of a Cs($6s$) + Cs($6p_{1/2}$) pair, at energies *above* the $(6s+6p_{1/2})$ threshold and *below* the $(6s+6p_{3/2})$ one, due to coupling between the continuum level and a bound level in the $0_u^+(6s+6p_{3/2})$ channel. The scattering resonance might then be stabilized by spontaneous emission towards the ground state of the molecule. A general scheme for the above mechanism is displayed in Figure 1.

A similar mechanism for dimer formation has long been known by experimentalists working, at thermal energies, with cells containing alkali atoms in presence of laser light: in the parity violation experiments of Bouchiat *et al.* [8,9] the presence of Cs_2 dimers [10] was interpreted as a coupling between a continuum level corresponding to a Cs($6s$) + Cs($6p_{3/2}$) collision in a repulsive potential, and bound levels in the well of excited molecular potential curves correlated to the above-lying $(6s+5d)$ dissociation limit. The aim of the present paper is to propose a theoretical investigation of such resonances and their stabilization by spontaneous emission, first at thermal energies and then in the cold regime.

In fact, the study of Feshbach resonances in a cold atom sample or in an atomic condensate is presently

[a] e-mail: francoise.masnou@lac.u-psud.fr

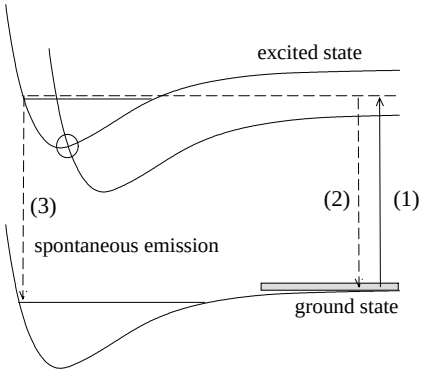

Fig. 1. General scheme of the formation of cold molecules by Feshbach resonances process. (1) Population of an atom in the excited state. Collisions between two atoms, one in the ground state and one in an excited state. (2) Spontaneous emission giving back two atoms in the ground state. (3) Population by spontaneous emission of a bound vibrational level of the molecular ground state.

a very active domain. However, most experimental and theoretical papers are focussed on magnetically-induced Feshbach resonances in collisions between two ground-state atoms, the stabilization process occurring when the magnetic field is modified [11–15]. Manipulation of Feshbach resonances by a time-dependent magnetic field has been theoretically investigated [16]. Optically-induced Feshbach resonances (where the continuum state of two ground-state colliding atoms is coupled by the light field to a vibrational level of a photoassociated molecule) have been observed by Fatemi *et al.* [17]. Feshbach resonances in ultracold atom-diatom scattering have been investigated by Forrey *et al.* [18,19]. The theoretical treatments are using close-coupling calculations [11,20], generalizing previous work on Feshbach resonances in molecular collisions at thermal energies: the subject of Feshbach resonances, and of predissociation of bound levels, has long been studied in molecular dynamics, for diatomic systems [21] as well as for triatomic van der Waals molecules [22,23]. Theoretical methods using optical potentials have been later on extensively developed [24–26].

Recently, a new kind of numerical method, based on Fourier grid expansion, has been developed for calculations of bound levels in diatomic molecules [27–30], and proved to be very efficient for highly-excited vibrational levels. It was generalized to the calculation of predissociation lifetimes by use of an optical potential [29,31,32]. In the present work, we propose an implementation of this approach to treat the formation of molecules by Feshbach resonances in an excited electronic state. The novel aspect relative to previous work lies upon the method chosen for the convergence checks and upon the determination of the wavefunctions.

The paper is organized as follows: in Section 2, we describe the numerical method to compute predissociation widths using Fourier Grid Hamiltonian representation and optical potential. This method is used in Section 3 in the case of Cs_2 dimers. In Section 4, we derive a formula giving an estimation of the rate of formation of molecules stabilized by spontaneous emission, relying upon knowledge of the predissociation width and spontaneous emission probability. In Section 5, we propose an application to the formation rate of Cs_2 molecules in a cell experiment at thermal energy. Further developments at ultracold energies are discussed in Section 6, and Section 7 is the conclusion.

2 The Fourier grid Hamiltonian representation (FGHR) and the optical potential method

The numerical method to solve the time-independent radial Schrödinger equation, known as Fourier Grid Hamiltonian representation (FGHR), has already been described in detail in several papers [27–29,33]. In the present work, we shall recall briefly its main lines and focus on its application when the Hamiltonian contains an optical potential. We propose a method to improve the optimization procedure for the optical potential.

2.1 The FGHR method

In the Fourier Grid method, we define a discretized basis set of N plane waves $\exp(\mathrm{i}2\pi kR/L)$, $k = -(N/2-1), ..., 0, ..., N/2$. L is the length of the grid in the position coordinate R and N the number of points. In a single channel problem, the wavefunctions for bound levels are represented by N expansion coefficients and the operators by $N \times N$ matrices. Diagonalization of the Hamiltonian matrix yields both the N eigenvalues and the N associated eigenvectors of the problem. Numerical checks must be performed to optimize the choice of the parameters L and N. One of the main advantages of the method is that it can be easily extended to many-closed-channel problems, the solution of a set of p coupled Schrödinger equation being reduced to diagonalization of a $pN \times pN$ matrix.

Moreover, in order to include open channels, where the continuum wavefunction is extending beyond the edge of any finite grid, the introduction of a complex absorbing potential, localized at the end of the grid to avoid unphysical reflections, is a very powerful numerical device [34].

As an example of two closed channels and one open channel, we consider two attractive potential curves $V_1(R)$ and $V_3(R)$ coupled to a repulsive potential $V_2(R)$ by interaction $W_{12}(R)$ and $W_{23}(R)$ respectively. R is the internuclear distance. In the present work we consider no rotational coupling effect, so that in the subspace of given total angular momentum J the Hamiltonian matrix is:

$$\mathbf{H} = \mathbf{T} + \mathbf{V} = \begin{pmatrix} T_1 & 0 & 0 \\ 0 & T_3 & 0 \\ 0 & 0 & T_2 \end{pmatrix} + \begin{pmatrix} V_1 & 0 & W_{12} \\ 0 & V_3 & W_{23} \\ W_{12} & W_{23} & V_2 - \mathrm{i}V_{\mathrm{opt}} \end{pmatrix} \quad (1)$$

where $\mathbf{T} = \frac{-\hbar^2}{2\mu}(\frac{\mathrm{d}^2}{\mathrm{d}R^2}) + \frac{\hbar J(J+1)}{2\mu R^2}$ and $\mathbf{V}$ are respectively the kinetic energy and potential operator and μ the reduced mass of the system. We assume that there is no coupling between the 2 attractive potentials, and consider a diabatic representation where the non-diagonal matrix elements of the kinetic energy operator can be neglected. $-\mathrm{i}V_{\mathrm{opt}}$ is the optical potential, that will be discussed below. Because of this complex term in the Hamiltonian matrix, diagonalization yields $3N$ complex eigenvalues expressed as:

$$\epsilon(v,J) = E_{v,J} - \mathrm{i}\frac{\Gamma_{v,J}}{2} \tag{2}$$

where $E_{v,J}$ and $\Gamma_{v,J}$ are respectively the position and width of the vibrational level v with rotational momentum J. The method is easy to implement and can be very accurate. The delicate part however is the implementation of the optical potential, for which the parameters (analytical expression, position, amplitude, width) must be optimized through numerical checks described below.

2.2 Choice of an optical potential

In previous papers computing resonances within an optical potential approach [24–26] and making use of a discrete variable representation [29,31], the authors studied the stability and the convergence of the computed widths with respect to the size L, number of points N of the numerical grid and the parameters of the optical potential (position, amplitude). In the present work we propose to add a further check studying the shape of the vibrational wavefunctions and of their Fourier transform. The latter procedure is made possible thanks to the FGHR method which provides wavefunctions both in position representation and in momentum representation. This allows a precise check of the wavefunction of a resonance, defined as a Siegert state in scattering theory [35].

Although the predissociation of a molecule is considering at least two channels, we shall first consider one channel scattering in order to define the physical concepts and present the optimization of an optical potential in a pedagogical way. Let us consider the radial Schrödinger equation describing the relative motion of two atoms in an interaction potential $U(R)$ with angular momentum l:

$$\left[\frac{\mathrm{d}^2}{\mathrm{d}r^2} - \frac{l(l+1)}{r^2} - \frac{2\mu}{\hbar^2}U(R) + k^2\right] y_{l,k}(R) = 0 \tag{3}$$

$\hbar k$ is the momentum related to the scattering energy E by $E = \hbar^2 k^2/2\mu$. We assume $U(R) \to 0$ as $R \to \infty$, $y_{l,k}(R)$ is the wavefunction for the l partial wave.

The asymptotic solution $y_{l,k}(R)$ of equation (3) can be developed over the ingoing and outgoing plane waves which are solution of the radial equation for a free particle as

$$y_{l,k}(R) \underset{R\to\infty}{\longrightarrow} f_l(k)\exp\left[-\mathrm{i}\left(kR - l\frac{\pi}{2}\right)\right] - f_l^*(k)\exp\left[\mathrm{i}\left(kR - l\frac{\pi}{2}\right)\right]. \tag{4}$$

The expansion coefficients $f_l(k)$ and $f_l^*(k)$ being the Jost functions, the scattering matrix S is defined as:

$$S_l(k) = \frac{f_l^*(k)}{f_l(k)}\,. \tag{5}$$

Resonances can be found as poles of the S matrix by considering complex values of the momentum k. From equation (5), such poles are found at zeros of the Jost function $f_l(k)$, where the wavefunction $y_{l,k}(R)$ becomes a purely outgoing wave

$$y_{l,k}(R) \underset{R\to\infty}{\longrightarrow} -f_l^*(k)\exp\left[\mathrm{i}\left(kR - l\frac{\pi}{2}\right)\right]. \tag{6}$$

In such a definition, bound states are associated with zeros of the Jost function $f_l(k)$ for k varying on the positive imaginary axis where the outgoing wave $\exp[\mathrm{i}(kR - l\pi/2)]$ becomes an exponentially decreasing function of the internuclear distance R. Resonances are associated with zeros of the Jost function for k varying in the lower half complex plane. Therefore, they correspond to a diverging outgoing wave well-known as Siegert state. The use of an optical potential solves the difficulty with their normalization. By introducing a dispersive term in the equation, it is possible to absorb the wavefunctions in the range where the complex potential is located. The solutions being exponentially decreasing at the very end of the grid, they become normalizable [24]. This is particularly interesting since continuum wavefunctions may be computed with the same accuracy as bound vibrational wavefunctions.

Therefore, we have to optimize an optical potential by ensuring that the wavefunction associated to a resonance becomes a purely outgoing wave. This can easily be checked by visualizing the Fourier transform of this wavefunction. We have illustrated this procedure by numerical calculations reported in Figure 2. Considering continuum levels at energy $\sim 10^{-4}$ a.u. above the dissociation limit of a Lennard-Jones potential $V(R) = C(A/R^{12} - B/R^6)$, where $A = 6$ and $B = 12$, $C = 3 \times 10^{-8}$ a.u., we have drawn the wavefunctions both in position and in momentum representation. When there is no optical potential (row (a)), the wavefunction is a standing wave represented by two symmetrical narrow peaks $(+k, -k)$ in the momentum representation. When the optical potential is well-optimized (row (c)), the wavefunction corresponding to a Siegert state displays an exponentially decreasing behavior at large distances, due to the strongly absorbing condition at the very end of the grid. In its Fourier transform, the peak corresponding to the ingoing wave has totally disappeared. In contrast, if the optimization is not satisfactory (row (b)), the incoming component is attenuated but not totally suppressed. The wavefunction

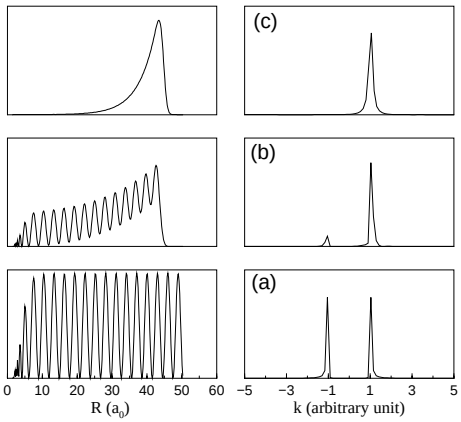

Fig. 2. Examples of waves functions (left) and their Fourier transform (right) computed with the Fourier grid method in the case of levels located above the dissociation limit of a Lennard Jones (12,6) potential (see text). Row (a) represents wavefunctions computed without optical potential. Row (b) shows the wavefunction for the same energy as previously but with an ill-adapted optical potential: the incoming wave is attenuated but not totally suppressed. Row (c) shows a wavefunction computed with a well-adapted optical potential, and representing a pure Siegert state. Note the exponentially decreasing long range behaviour and the total suppression of the ingoing wave.

displays some residual oscillations due to unphysical reflection at the edge of the grid, as well as an exponentially diverging behavior at large distances.

We may conclude that the suppression of the peak at $k < 0$ in the Fourier transform appears as a very convenient convergence check. In the absence of optical potential, a reduction of the grid step for given L results in a higher density of continuum levels, with no improvement for the accuracy of the results. On the other hand, with an optical potential we can identify stable levels above the dissociation limit and the acurracy in the computed position and width improves when increasing the number of grid points.

Practically, we add this supplementary check to the usual requirements for a "good" optical potential already described in references [25,29], namely the location at a distance $R \sim R_0$ far enough in the asymptotic region in order to avoid perturbation in the physical interaction area and the choice of a smooth variation of $V_{\rm opt}(R)$ to avoid unphysical reflections. The best choice for the function $V_{\rm opt}(R)$ is well-analysed in the article of Vibók and Balint-Kurti [34], from where we took

$$V_{\rm opt} = A_5 N_{\rm opt} \exp\left(\frac{-2L_{\rm opt}}{R - R_{\rm opt}}\right), \qquad (7)$$

with $A_5 = 0.006$ a.u., $L_{opt} = 3$ a.u. The optical potential starts at a distance $R_{\rm opt}$ which we have chosen as $R_{\rm opt} = L - L_{\rm opt}$ for a grid of length L.

We did verify that the use of a quadratic potential gives the same result. In the following we shall consider reactions where the angular momentum is conserved, so that $l = J$.

3 Application to the predissociation of the $C^1\Pi_u(6s + 5d)$ state of the Cs_2 dimers

A very efficient and long known [36,37] predissociation scheme of the Cs_2 dimers occurs for the rovibrational levels of the attractive $C^1\Pi_u(6s+5d)$ state which is coupled *via* spin-orbit coupling to the dissociative $(2)^3\Sigma_u^+(6s+6p)$ state. The inverse reaction is a Feshbach resonance in the scattering of a ground state atom and an excited one in the $(2)^3\Sigma_u^+(6s+6p)$ potential:

$$\begin{aligned} {\rm Cs}(6s) + {\rm Cs}(6p) + E &\rightarrow {\rm Cs}_2^*((2)^3\Sigma_u^+(6s+6p))(E, l = J) \\ &\rightarrow {\rm Cs}_2^*(C^1\Pi_u(6s+5d))(v, J) \end{aligned} \qquad (8)$$

which can be stabilized by spontaneous emission

$$\begin{aligned} {\rm Cs}_2^*(C^1\Pi_u(6s+5d), v, J) \rightarrow \\ {\rm Cs}_2(X^1\Sigma_g^+(6s+6s)v", J") + h\nu. \end{aligned} \qquad (9)$$

The energy origin is taken at the $(6s + 6p)$ dissociation limit. This reaction at room temperature has been observed by Bouchiat and Lintz as an efficient channel for dimer formation in their parity violation experiment [10].

We have applied the previous method to numerical calculations of the predissociation effect, eventually considering a third channel, $(2)^3\Pi_u(6s + 5d)$ also coupled to $(2)^3\Sigma_u^+(6s + 6p)$, so that in the Hamiltonian H in equation (1) the potentials $V_1(R)$, $V_2(R)$ and $V_3(R)$ correspond respectively to the electronic states $C^1\Pi_u(6s+5d)$, $(2)^3\Sigma_u^+(6s + 6p)$ and $(2)^3\Pi_u(6s + 5d)$. We have used the Hund case (c) adiabatic potentials from Aubert-Frécon *et al.* [38], which are computed up to $R = 140$ a.u. We found a few discrepancies between those curves and the earlier calculations of Spies and Meyer [39], which are limited to distances $R \leq 30$ a.u. In the latter case, in contrast with the curves computed by the same authors for the $6s + 6p$ manifold, the matching with long range asymptotic curves, computed for instance from the multipole coefficients of Marinescu and Dalgarno [40] is not easy. Details will be given in a forthcoming publication. In order to deal with diabatic states, we performed a diabatization procedure of the Hund case (c) curves and we modelled the spin-orbit interaction by a Gaussian function localized at the crossing point of the potentials

$$W(R) = W_{\rm int} \exp\left(-\frac{(R - R_{\rm int})^2}{\omega^2}\right) \qquad (10)$$

where $W_{\rm int}$ is the interaction strength equal to half the splitting between the adiabatic potentials. $R_{\rm int}$ is the position of the crossing point and ω is the width of the Gaussian interaction. The parameters in the model are chosen so that when diagonalizing the diabatic matrix $\mathbf{V}(R)$ in equation (1), we get back the adiabatic curves. The optimized parameters are $W_{\rm int} = 1.75\times10^{-4}$ a.u., $\omega = 0.3$ a.u. and $R_{\rm int} = 9.7$ a.u. for $W_{12}(R)$ and $W_{\rm int} = 3.5\times10^{-4}$ a.u., $\omega = 0.6$ a.u. and $R_{\rm int} = 11.6$ a.u., for $W_{23}(R)$. The three diabatic potentials are represented in Figure 3, while the coupling terms are displayed in Figure 4. We put the

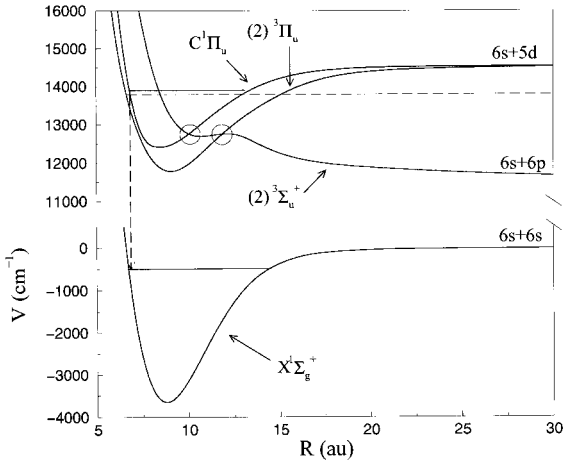

Fig. 3. Diabatic potentials $V_1(R), V_2(R)$ and $V_3(R)$ in the case of cesium dimer. The $C^1\Pi_u(6s{+}5d)$ and $(2)^3\Pi_u(6s{+}5d)$ states predissociate through the dissociative $(2)^3\Sigma_u^+(6s+6p)$ state. The picture also shows the formation scheme for molecules in the ground $X^1\Sigma_g^+(6s{+}6s)$ state by spontaneous emission *via* a Feshbach resonance due to the spin-orbit interaction between the excited electronic states.

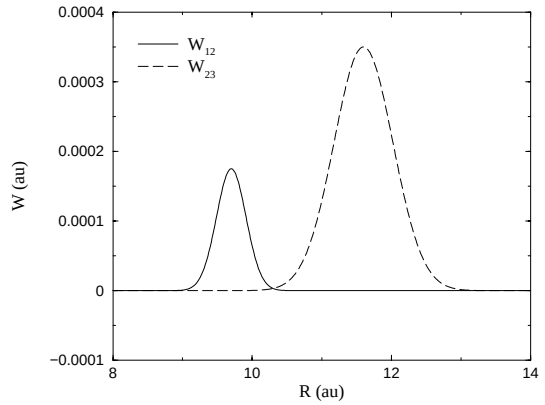

Fig. 4. Representation of the coupling terms, modelized by a Gaussian curve (see Eq. (10) in text). Solid line: interaction $W_{12}(R)$ between the $C^1\Pi_u$ and the $(2)^3\Sigma_u^+(6s{+}6p)$ potentials. Dashed line; interaction $W_{23}(R)$ between the $(2)^3\Pi_u(6s+5d)$ and the $(2)^3\Sigma_u^+(6s+6p)$ potentials.

absorbing potential $-\mathrm{i}V_{\mathrm{opt}}$ on the open channel, at a distance $R_{\mathrm{opt}} = 30$ a.u., in a region where the $(2)^3\Sigma_u^+(6s{+}6p)$ curve has reached its dissociation limit. We first have made two channel calculations considering $W_{23}(R) = 0$. The optimization of the optical potential follows the method described in the preceeding section, a typical example of a resonant wavefunction being represented in Figure 5.

The energies and widths for the levels of the $C^1\Pi_u(6s{+}5d)$ vibrational series, predissociated by the $(2)^3\Sigma_u^+(6s+6p)$ channel, have been computed for various values of the grid length L, and are displayed in Figure 6. The widths display an oscillatory pattern characteristic of such molecular dynamics, as discussed by Lefebvre-Brion and Field [21]. When the energy E is varying, the overlap integral between the bound and the continuum wavefunction is oscillating due to the variation of their relative phase.

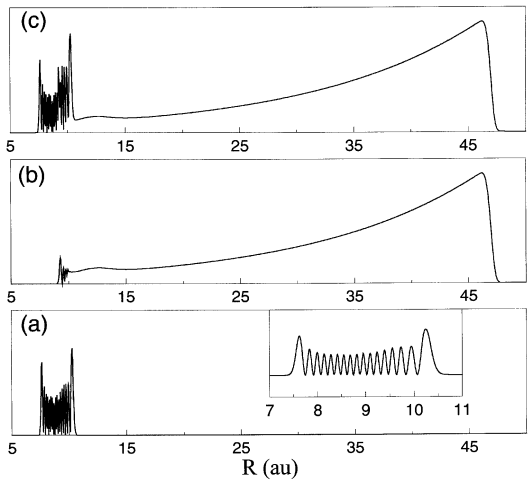

Fig. 5. Representation of the wavefunction associated with the 17th predissociated vibrational level of the $C^1\Pi_u$ state in a two state model. The picture (a) shows the component on the $|C^1\Pi_u\rangle$ state and the picture (b) shows the component on the dissociative $|^3\Sigma_u^+\rangle$ state. The first is a vibrational level whereas the second is a continuum state with a pure divergent behavior. The criterion based on the shape of the wave function and its Fourier transform is equivalent to the tests of Monnerville *et al.* [29], indeed with the use of the same optical potential,we check that the widths have converged by increasing the length L of the numerical grid. Picture (c) shows the total wave function.

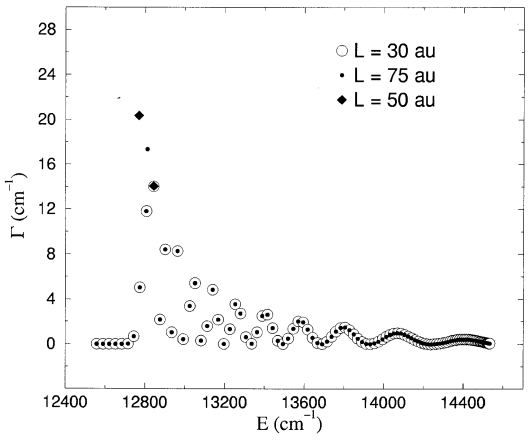

Fig. 6. Positions and widths for the $C^1\Pi_u$ vibrational levels predissociated by the $^3\Sigma_u^+(6s+6p)$ state. Values are reported for two choices of the grid length, showing the stability of the results. Diamonds show values for intermediate grid length for two levels which are not really converged. For these two levels, stability can not be reached because they are located flush with the avoided crossing of the potentials and are very strongly perturbated by the interaction.

The convergence is rapid, the results being equivalent for grid lengths $L = 30$, 50 and 70 a.u., apart from a markedly predissociated level at $E = 12\,810\ \mathrm{cm}^{-1}$ for which the continuum component in the wavefunction is so important that a grid of length $L > 70$ a.u. is required.

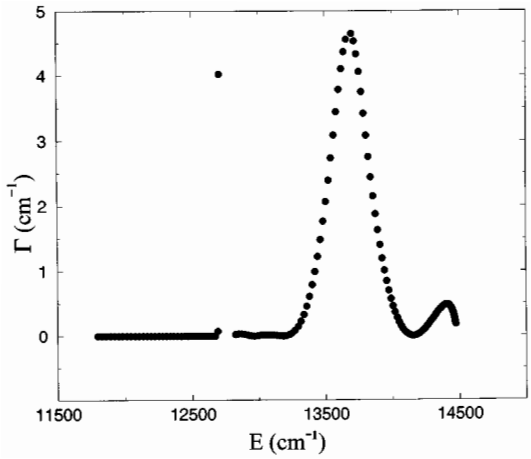

Fig. 7. Positions and widths for the $^3\Pi_u(6s+5d)$ vibrational levels predissociated by the $^3\Sigma_u^+(6s+6p)$ continuum.

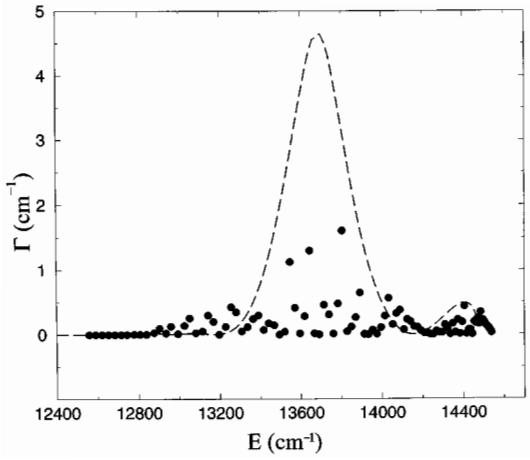

Fig. 8. Positions and widths for the $C^1\Pi_u$ vibrational levels in a 3-channel calculation including both the $^3\Sigma_u(6s+6p)$ and the $^3\Pi_u(6s+5d)$ channels. The shape of the peak in Figure 7 is recalled in the broken curve.

We have also computed, within a two-channel model, the predissociation widths for the $(2)^3\Pi_u$ levels predissociated by the $(2)^3\Sigma_u^+(6s+6p)$ channel (see Fig. 7). In the latter case, the dynamics is different: a broad peak is present around 13 700 cm^{-1}, and the energy variation of the predisssociation width does not display the oscillating pattern discussed in the previous case. The qualitative difference between Figures 6 and 7 can be explained by the different energy dependence of the overlap integrals between the continuum function at energy E and bound functions in the two potentials. Indeed, the potential $C^1\Pi_u(6s+5d)$ is less deep than the $(2)^3\Pi_u(6s+5d)$ potential. These overlap integrals have also been calculated by Kimura *et al.* [41] who show clearly the different energy variation.

Next we have performed three-channel calculations, for which the results are displayed in Figure 8. The patterns of the two preceeding figures are mixed, with oscillations as in Figure 6 and some large values of the width in the region of the broad peak in Figure 7. However, it is remarkable that when we take into account the $(2)^3\Pi_u(6s+5d)$ channel, the widths are reduced by one order of magnitude as compared to Figure 6. This shows the importance of introducing this third channel in the treatment. The qualitative explanation is easy: for the lowest energies, the coupling with the $(2)^3\Pi_u(6s+5d)$ channel is weak, as is manifested in Figure 7, so that the resonant structure is very similar to the 2-state calculations of Figure 6, the effect of third channel being only manifested by a decrease in the lifetimes. Above the energy $E = 13\ 200$ cm^{-1}, the coupling with the $(2)^3\Pi_u(6s+5d)$ channel becomes important, and large predissociation lifetimes are found in the region of the peak in Figure 6. Interference effects between the two predissociated series have also been observed in the calculations of Kimura *et al.* [41]

The validity of the present model is restricted to non overlapping resonances: it can be easily verified that the computed widths are smaller than the level spacing. In our case, the ratio between the spacing and the width is always larger than 5.

In a model where no rotational coupling is introduced, the calculations can be performed for various values of the angular momentum J, by considering the J dependence of the potentials and kinetic energy, yielding a set of energies and widths $E_{v,J}$ and $\Gamma_{v,J}$. We have checked that the *J-dependence* of the results is weak, the widths $\Gamma_{v,J}$ varying by less than 10% when the rotational number increases from 0 to 50.

4 Molecular formation rate by stabilization of Feshbach resonances in an excited sate

4.1 general expression for the rate coefficient

The predissociation of the bound rovibrational levels described in the previous section is the inverse process of a Feshbach resonance in the scattering of two Cs($6s$) + Cs ($6p$) atoms at a collision energy E, for an angular momentum J. The analytic expression for the elastic scattering matrix **S** in the case of an isolated resonance is [7]

$$S_{ii}^v(E,J) = F_{ii}^v\left(1 - \frac{\mathrm{i}\Gamma_{v,J}}{E - E_{v,J} + \frac{\mathrm{i}}{2}\Gamma_{v,J}}\right), \qquad (11)$$

where E is the initial collisional energy, $E_{v,J}$ and $\Gamma_{v,J}$ respectively the position and the width of a resonance, and F_{ii}^v is a phase factor, such that $|F_{ii}^v|^2 = 1$. The widths Γ_v that we have computed range from 0 to 15 cm^{-1}, corresponding to lifetimes between 0.35 ps and ∞. When the radiative lifetime is much larger than the predissociation lifetime, the spontaneous emission to the ground electronic state $X^1\Sigma_g^+(6s+6s)$ can be introduced phenomenologically by a small additive term to the imaginary part of the complex energy, which now becomes $E_{v,J} - \mathrm{i}\Gamma_{v,J}/2 - \mathrm{i}\gamma_{v,J}/2$, with $\gamma_{v,J} \ll \Gamma_{v,J}$ [42]. The S matrix element for scattering in the initial channel becomes:

$$S_{ii}^v(E,J) = F_{ii}^v\left(1 - \frac{\mathrm{i}\Gamma_{v,J}}{E - E_{v,J} + \frac{\mathrm{i}}{2}\gamma_{v,J} + \frac{\mathrm{i}}{2}\Gamma_{v,J}}\right)\cdot \qquad (12)$$

The squared modulus of this matrix element is no longer 1 but,

$$|S^v_{ii}(E,J)|^2 = \frac{(E-E_{v,J})^2+(\gamma_{v,J}-\Gamma_{v,J})^2/4}{(E-E_{v,J})^2+(\gamma_{v,J}+\Gamma_{v,J})^2/4} < 1. \quad (13)$$

The fact that in equation (13) $|S^2_{ii}|^2 < 1$ manifests a flux loss in the scattering channel. When the spontaneous decay is preferentially populating bound levels of the ground electronic state, this flux loss will give the rate of formation of ground state molecules. In the other cases, it will give an upper limit of the latter quantity. Writing the flux conservation condition as

$$|S^v_{ii}(E,J)|^2 + |S^v_{\rm decay}(E,J)|^2 = 1, \quad (14)$$

yields, when decay to the continuum of the ground state may be neglected, a probability for the formation of stable molecules:

$$|S^v_{\rm decay}(E,J)|^2 = \frac{\gamma_{v,J}\Gamma_{v,J}}{(E-E_{v,J})^2+\left(\frac{\gamma_{v,J}+\Gamma_{v,J}}{2}\right)^2}\cdot \quad (15)$$

We can thus define a stabilization cross-section as:

$$\sigma^v_{\rm decay}(E) = \frac{\pi}{2\mu E}\sum_{J=0}^{\infty}(2J+1)|S^v_{\rm decay}(E,J)|^2, \quad (16)$$

from which the rate coefficient at a temperature T for the molecular formation process is obtained by averaging over the velocity distribution $f(w,T)$,

$$K(v,T) = \int_0^\infty \sigma^v_{\rm decay}(E) w f(w,T) {\rm d}w. \quad (17)$$

In equation (17), w is the modulus of the relative velocity of the colliding particles. For cell experiments, we consider a Maxwellian velocity distribution [43]

$$f^{\rm Max}(w,T) = \left(\frac{2\mu^3}{\pi k_{\rm B}^3 T^3}\right)^{\frac{1}{2}} w^2 \exp\left(-\frac{\mu w^2}{2k_{\rm B}T}\right), \quad (18)$$

where $k_{\rm B}$ is the Boltzman constant. Introducing the change of variable: $E = (1/2)\mu w^2$, $w{\rm d}w = {\rm d}E/\mu$ and combining equations (16, 18), to equation (17), the rate of formation of stable molecules, at a temperature T, from a given resonance v is obtained as a sum over the energy-averaged decay probabilities for the various partial waves:

$$K(v,T) = \frac{1}{hQ_T}\sum_{J=0}^{\infty}(2J+1) \times \int_0^\infty |S^v_{\rm decay}(E,J)|^2 \exp\left(-\frac{E}{k_{\rm B}T}\right){\rm d}E \quad (19)$$

where we have introduced the partition function $Q_T = (2\pi\mu k_{\rm B}T/h^2)^{3/2}$.

At thermal energies, the resonances are usually very narrow in comparison with $k_{\rm B}T$, so that the exponential term can be taken out of the integral. Due to the Lorentzian shape of the probability in equation (15), the remaining integration is analytical, and one obtains the total rate of formation of molecules by summation over the various resonances as:

$$K^{\rm tot}(T) \sim \sum_v \frac{1}{hQ_T}\sum_{J=0}^{\infty}(2J+1)\frac{2\pi\gamma_{v,J}\Gamma_{v,J}}{\gamma_{v,J}+\Gamma_{v,J}}\exp\left(-\frac{E_{v,J}}{k_{\rm B}T}\right). \quad (20)$$

Note that under the condition $\gamma_{v,J} \ll \Gamma_{v,J}$, the formation rate is controlled by the spontaneous emission probability and by the energy distribution of the resonances. This simple analytical formula is no longer valid in the cold regime, where numerical calculations have to be performed.

The width $\gamma_{v,J}$ that we have phenomenologically introduced is related to the probability of spontaneous emission from one rovibrational level v, J in the excited molecular state Λ to all possible rovibrational levels v'', J'' in the ground electronic state Λ''. The Einstein coefficient for transition to a particular v'', J'' level may be written [44]:

$$A_{vJ\to v''J''} = \frac{1}{4\pi\epsilon_0}\frac{64\pi^4}{3hc^3}\nu^3_{vJ\to v''J''}D_{\Lambda vJ\to\Lambda''v''J''}. \quad (21)$$

In equation (21) $\nu_{vJ\to v''J''}$ is the frequency of the transition, and

$$D_{\Lambda vJ\to\Lambda''v''J''} = \sum_M\sum_{M''}|\langle \Lambda vJM|\mu(\mathbf{R})|\Lambda''v''J''M''\rangle|^2. \quad (22)$$

$\mu(\mathbf{R})$ is the electric dipole moment, and can be expressed from its three components μ_x, μ_y and μ_z as tensor of rank 1:

$$\mu^{(1)}_{\pm1}(R) = \frac{\mu_x(R) \pm {\rm i}\mu_y(R)}{\sqrt{2}}, \quad (23)$$

$$\mu^{(1)}_0(R) = \mu_z(R). \quad (24)$$

where the three subscripts x, y, z denote the components of the dipole vector in the molecular frame.

For a simple estimation, we shall neglect the R-dependence of the dipole moment [21], and assume that the J distribution is narrow enough to neglect the variation of the radial wavefunction with the rotational quantum number [45]. The dipole integral in equation (22) can then be separated into radial part and angular part, and after summation over the J'' quantum number in the final state, the J number vanishes, so that after some algebraic manipulation we have:

$$\sum_{J"} A_{vJ\to v''J''} \sim A_{v\to v''} \quad (25)$$

$$\approx \frac{1}{4\pi\epsilon_0}\frac{64\pi^4}{3h}\frac{\nu^3}{c^3}|\langle v|\mu|v''\rangle|^2(2-\delta_{\Lambda 0}\delta_{\Lambda''0}), \quad (26)$$

where $\delta_{\Lambda 0} = 1$ for Σ states, and 0 otherwise.

The natural width due to spontaneous emission is then found J-independent and reads

$$\gamma_v \sim \hbar\sum_{v''} A_{v'\to v''}. \quad (27)$$

5 Application to an estimation of the formation rate of ground state Cs_2 molecules at thermal energies

We focus on the excited molecules in the $C^1\Pi_u(6s + 5d)$ electronic state which decay by spontaneous emission into the ground $X^1\Sigma_g^+(6s + 6s)$ state. Due to selection rules for $\Pi-\Sigma$ transition, only the ±1 components of the tensor are contributing to equation (21). Numerical calculations show that the probability of decay by spontaneous emission into the continuum of the $X^1\Sigma_g^+(6s+6s)$ state is close to zero. Because of selection rules, the Cs $6s \rightarrow 5d$ transition is forbidden. The molecular $C^1\Pi_u(6s + 5d) \rightarrow X^1\Sigma_g^+(6s + 6s)$ transition dipole moment is presently unknown. Earlier spectroscopic studies of the $C^1\Pi_u(6s + 5d)$ spectra [46] obtained by population from the ground state demonstrate that it is easy to transfer population. To estimate the molecular rate, we have taken the only known dipole moment [39] for a similar transition $((2)^3\Pi_g(6s+5d) \rightarrow a^3\Sigma_u^+(6s+6s))$ averaged over the range of the rovibrational levels of the $C^1\Pi_u(6s+5d)$ state providing a constant dipolar moment of the order of 1 au which can be taken out of the integral in equation (22) (by comparison, the dipole moment for the $6s$–$6p$ atomic transition is 3.236 a.u.) The calculation of the natural width is then easily done.

The sum of the overlap integrals between one excited vibrational state v and the ground vibrational states v'' is numerically found equal to one, justifying *a posteriori* the hypothesis neglecting bound $\rightarrow$ continuum transitions. We can safely assume that the natural width due to spontaneous emission is constant for all the vibrational levels ($\gamma_v = \gamma$), yielding a natural width of 6.6×10^{-5} cm^{-1}. For numerical convenience, we compute positions and widths of the resonances for a given J number and we expressed a total rate (that is summed over all the resonances) for each J. This is equivalent to performing in equation (20) the summation over v before the summation over J

$$K^{\rm tot}(T) = \sum_{J=0}^{\infty} \kappa_J^{\rm tot} \tag{28}$$

$$\kappa_J^{\rm tot}(T) = \sum_v \frac{1}{hQ_T}(2J+1)\frac{2\pi\gamma\Gamma_{v,J}}{\gamma+\Gamma_{v,J}} \exp\left(-\frac{E_{v,J}}{k_{\rm B}T}\right). \tag{29}$$

The J-dependence of the partial rate $\kappa_J^{\rm tot}(T)$ at room temperature is displayed below in Figure 9, in a model using for the widths $\Gamma_{v,J}$ numerical results from two-channel calculations. The derivation in Section 4 is considering only $(2)^3\Sigma_u^+(6s + 6p)$ continuum and $C^1\Pi_u(6s + 5d)$ bound levels. We then find, for a temperature of 300 K, a total molecular formation rate of $3\times10^{-18}\times\langle d\rangle^2$ cm^3 s^{-1}, where $\langle d\rangle^2$ is the actual value of the dipole moment in atomic units. This illustrates the possible efficiency of such a scheme at room temperature. The rate is substantially improved by the fact that at room temperature the Maxwell distribution is very broad and many resonances (up to 100) are populated and contribute. On the other hand,

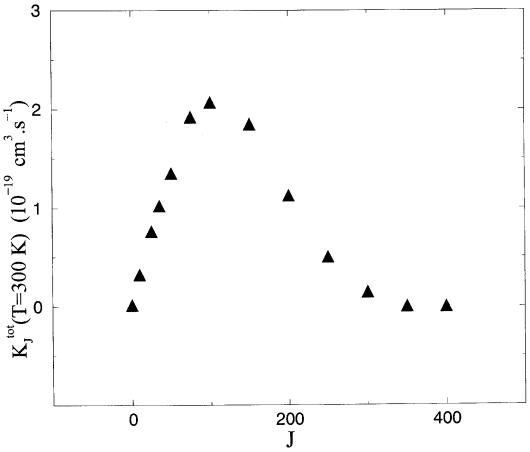

Fig. 9. Molecular partial formation rate $\kappa_J(T)$ (see Eq. (29)) in cm^{3}s^{-1} *versus* the rotational quantum number J for $T =$ 300 K.

because of the repulsive character of the $(2)^3\Sigma_u^+(6s+6p)$ curve and of the location of the minimum of the C curve the rate decreases dramatically as the temperature of the vapor decrease: the rate is 4 order of magnitude smaller for a temperature of 100 K, and is close to zero at 50 K. This is due to the fact that the resonances are located in the exponentially decreasing range of the Maxwellian velocity distribution which tends quickly to zero as the temperature tends to zero.

The number of molecules formed per second will depend upon the density of atoms in the ground and in the excited state, and of the volume of the cell. Considering typical densities of 10^{14} cm^{-3} and 10^{10} cm^{-3} for atoms in the ground and in the excited state respectively and cell volume of 1 cm^3, the number of molecules formed by spontaneous emission reaches 3×10^6 s^{-1} with our arbitrary choice for the dipole moment.

We should note that the rate computed using the numerical values obtained in a three-channel calculation do not differ substantially from the previous ones. Indeed, the rate is only reduced by 20% for a temperature of 300 K. This can be explained from formula (20) due to the small value of $\gamma_{v,J}$ as compared to $\Gamma_{v,J}$.

6 Possible application to cold collisions

In the cold regime, we should first look for situations as in Figure 1 where in the initial continuum channel the potential is attractive at long range, and where in the predissociated channel the potential is deep enough so that bound levels may exist at energy $E \approx k_{\rm B}T$. A similar situation is offered by considering a collision Cs($6s$) + Cs($6p_{1/2}$) along the $0_u^+(6s+6p_{1/2})$ potential curve and studying the possibility of a Feshbach resonance with a bound level in the Cs_2 $0_u^+(6s + 6p_{3/2})$ curve. The strong coupling of the two channels, also present in the Rb_2 $0_u^+(5s + 5p_{1/2,3/2})$ case, gives rise to strong predissociation effects: the computed widths [32] close to the $p_{1/2}$ asymptote are typically

of the same order of magnitude as the widths calculated in Section 5, varying from 2.5 cm^{-1} for $^{85}Rb_2$, 0.8 cm^{-1} for $^{87}Rb_2$ and 0.15 cm^{-1} for Cs_2. Once populated, the vibrational levels in the $0_u^+(6s + 6p_{3/2})$ curve have been shown to decay efficiently into bound levels of the ground state [6], so that the stabilization by spontaneous emission would be an efficient process. However, in the cold regime the very existence of a Feshbach resonance is problematic: the Maxwell distribution becomes very narrow, and below a temperature of a few kelvins is even narrower than the spacing between two resonances. Finding a resonance located exactly at the peak in the energy distribution is purely fortuitous: for instance, the lower resonance in the Cs_2 $0_u^+(6s + 6p_{3/2})$ channel is located ≈ 2 cm^{-1} above the $(6s + 6p_{1/2})$ threshold, and cannot be reached during $Cs(6s)$ + $Cs(6p_{1/2})$ collisions at ultracold temperatures. The first condition would be to design a process allowing to control the position of the resonance, for instance *via* laser coupling [47–49]. If this can be achieved, the rate in the previous section should be computed numerically, the analytical approximation on the integral over energy distribution being no longer justified. We may predict however that going to low temperatures, the limitation in the number of resonances and also in the number of partial waves (factor $J_{\max}^2$) is decreasing the formation rate. In contrast, the geometrical factor E^{-1} in equation (16) increases the rate, so that the balance between the two effects suggests a substantial increase of the formation rate.

The advantage of such a procedure compared to resonances in the ground state controlled by magnetic field is that the spontaneous emission is populating low vibrational levels of the ground electronic state, so that the stable molecules are produced vibrationally cold.

7 Conclusion

In the present work we have proposed a theoretical method to compute predissociation widths and Feshbach resonances of excited alkali dimers in the framework of a Fourier Grid representation with optical potential. We also have presented a phenomenological treatment of the stabilization of such Feshbach resonances by spontaneous emission.

Calculations for the predissociation of the Cs_2 $C^1\Pi_u(6s + 5d)$ vibrational levels by the $^3\Sigma_u(6s + 6p)$ continuum show that the interpretation of dimer formation, observed in the experiment of Lintz and Bouchiat, by Feshbach resonances is qualitatively correct. The pairs of atoms $Cs(6s)$ + $Cs(6p)$ colliding along the $^3\Sigma_u(6s+6p)$ potential are likely form a $C^1\Pi_u(6s+5d)$ resonance. The latter having a favourable Franck Condon overlap with the bound levels of the ground state are good candidates for stabilization *via* spontaneous emission. For a quantitative comparison, values of the electronic transition dipole moment between the two molecular states are necessary.

More elaborate calculations would necessitate a more refined treatment of the spontaneous emission step. Besides, we have considered a constant population of excited atoms due to the presence of a cw laser and this coupling with light should also be introduced in our model. It might be interesting to consider generalization of such a process to cold collisions, provided experiments could be easily implemented to tune the position of the resonances with laser light. The advantage of the proposed scheme is twofold. First, in contrast with photoassociation many atoms can be excited with resonant light, creating a large number of colliding pairs $A(ns)$ + $A(np)$ likely to contribute to the resonance. Second, in contrast with the Feshbach resonances in the ground state tuned by magnetic field the present scheme can transfer population to the lower vibrational levels of the ground state.

Discussions with M.A. Bouchiat and C. Dion are gratefully acknowledged. The authors are grateful to M. Aubert-Frécon and to W. Meyer for making their computed potential curves available and to C. Amiot for indicating spectroscopic references. P.P. wishes to thank E. Luc-Koenig and M. Millet for useful references and comments. F.M.S. thanks ITAMP and its staff for hospitality in Cambridge where this paper was partly written. IDRIS computing center (France) where the calculations were performed, is gratefully acknowledged.

References

1. A. Fioretti, D. Comparat, A. Crubellier, O. Dulieu, F. Masnou-Seeuws, P. Pillet, Phys. Rev. Lett. **80**, 4402 (1998)
2. T. Takekoshi, B.M. Patterson, R.J. Knize, Phys. Rev. Lett. **81**, 5105 (1999)
3. N. Nikolov, E.E. Eyler, X.T. Wang, J. Li, H. Wang, W.C. Stwalley, Ph. Gould, Phys. Rev. Lett. **82**, 703 (1999)
4. C. Gabbanini, A. Fioretti, A. Lucchesini, S. Gozzini, M. Mazzoni, Phys. Rev. Lett. **84**, 2814 (2000)
5. H.R. Thorsheim, J. Weiner, P.S. Julienne, Phys. Rev. Lett. **58**, 2420 (1987)
6. C.M. Dion, C. Drag, O. Dulieu, B. Laburthe Tolra, F. Masnou-Seeuws, P. Pillet, Phys. Rev. Lett. **86**, 2253 (2001)
7. H. Feshbach, *Theoretical Nuclear Physics* (Wiley and sons, New York, 1992)
8. M.A. Bouchiat, J. Guéna, L. Hunter, L. Pottier, Phys. Lett. B **117**, 358 (1982)
9. M.A. Bouchiat, C. Bouchiat, Rept. Prog. Phys. **60**, 1351 (1997)
10. M. Lintz, M.A. Bouchiat, Phys. Rev. Lett. **80**, 2570 (1998)
11. A. Axelsson, A.J. Moerdijk, B.J. Verhaar, Phys. Rev. A **51**, 4852 (1995)
12. F.A. van Abeleen, D.J. Heinzen, B.J. Verhaar, Phys. Rev. A **57**, R4102 (1998)
13. Ph. Courteille, R.S. Freeland, D.J. Heinzen, F.A. van Abeleen, B.J. Verhaar, Phys. Rev. Lett. **81**, 69 (1998)
14. Ch. Chin, V. Vuletić, A.J. Kerman, S. Chu, Phys. Rev. Lett. **85**, 2717 (2000)
15. P.J. Leo, C.J. Williams, P.S. Julienne, Phys. Rev. Lett. **85**, 2721 (2000)
16. F.H. Mies, E. Tiesinga, P.S Julienne, Phys. Rev. A **61**, 022721–1 (2000)
17. F.K. Fatemi, K.M. Jones, P.D. Lett, Phys. Rev. Lett. **85**, 4462 (2000)

18. R.C. Forrey, N. Balakrishnan, A. Dalgarno, M.R. Haggerty, E.J. Heller, Phys. Rev. Lett. **82**, 2657 (1999)
19. R.C. Forrey, V. Karchenko, N. Balakrishnan, A. Dalgarno, Phys. Rev. A **59**, 2146 (1999)
20. F.H. Mies, C.J. Williams, P.S. Julienne, M. Krauss, J. Res. Natl. Inst. Stand. Technol. **1001**, 521 (1996)
21. H. Lefebvre-Brion, R.W. Field (Academic Press, New York, 1986)
22. J.A. Beswick, J. Jortner, J. Chem. Phys. **68**, 2277 (1978)
23. S.K. Gray, S.A. Rice, J. Chem. Phys. **83**, 2818 (1985)
24. G. Jolicard, E.J. Austin, Chem. Phys. Lett. **121**, 106 (1985)
25. E.J. Austin, G. Jolicard, Chem. Phys. **103**, 295 (1986)
26. C. Leforestier, E.J. Austin, G. Jolicard, J. Chem. Phys. **88**, 1026 (1988)
27. C.C. Marston, G. Balint-Kurti, J. Chem. Phys. **91**, 3571 (1989)
28. D.T. Colbert, W.H. Miller, J. Chem. Phys. **96**, 1982 (1992)
29. M. Monnerville, J.M. Robbe, J. Chem. Phys. **101-112**, 7580 (1994)
30. V. Kokoouline, O. Dulieu, R. Kosloff, F. Masnou-Seeuws, J. Chem. Phys. **110**, 9865 (1999)
31. M. Monnerville, J.M. Robbe, Eur. Phys. J. D **5**, 381 (1999)
32. V. Kokoouline, O. Dulieu, R. Kosloff, F. Masnou-Seeuws, Phys. Rev. A **62**, 032716 (2000)
33. O. Dulieu, P.S. Julienne, J. Chem. Phys. **103**, 60 (1995)
34. Á. Vibók, G.C. Balint-Kurti, J. Phys. Chem. **96**, 8712 (1992)
35. J.R. Taylor, *Scattering Theory* (Wiley and sons, New York, 1977)
36. S. Kasahara, Y. Hasui, K. Otsuka, M. Baba, W. Demtröder, H. Katô, J. Chem. Phys. **106**, 4869 (1997)
37. S. Kasahara, K. Otsuka, M. Baba, H. Katô, J. Chem. Phys. **109**, 3393 (1998)
38. M. Aubert-Frécon, private communication
39. N. Spies, Ph.D. thesis, Fachbereich Chemie, Universität Kaiserslautern, 1989
40. M. Marinescu, A. Dalgarno, Phys. Rev. A **52**, 311 (1995)
41. Y. Kimura, H. Lefebvre-Brion, S. Kasahara, H. Katô, M. Baba, R. Lefebvre, J. Chem. Phys. **113**, 8637 (2000)
42. C. Cohen-Tannoudji, B. Diu, F. Laloë, *Mécanique quantique* (Hermann, Paris, 1977)
43. B. Diu, *Physique Statistique* (Hermann, Paris, 1989)
44. D.C. Morton, L. Noreau, Astrophys. J. **95**, 301 (1994)
45. M.-L. Almazor, O. Dulieu, F. Masnou-Seeuws, J. Mol. Spec. **191**, 81 (1998)
46. M. Raab, G. Höning, C.R. Vidal, W. Demtröder, J. Chem. Phys. **76**, 4370 (1982)
47. P.O. Fedichev, Y. Kagan, G.V. Shlyapnikov, J.T.M. Walraven, Phys. Rev. Lett. **77**, 2913 (1996)
48. M. Vatasescu, O. Dulieu, R. Kosloff, F. Masnou-Seeuws, Phys. Rev. A **63**, 033407 (2001)
49. V. Kokoouline, J. Vala, R. Kosloff, J. Chem. Phys. **114**, 3046 (2001)